Supporting Information

Ferry et al. 10.1073/pnas.1102572108

SI Materials and Methods

Plasmids and Reagents. The B10-HA-FLAG–tagged SRC-3 and RARα vectors and the DR5-tk-CAT reporter gene were described (1, 2). The expression vectors for SRC-3 S505A, S543A, S860A, and S867A were constructed by cloning the cDNA of the corresponding mutants provided by B. W. O'Malley (Baylor College of Medicine, Houston, TX) into a pTL2 vector containing a FLAG-tag. The pCDNA-based expression vectors for CUL-1, CUL-2, and CUL-3 with an HA tag were kindly provided by W. Krek (Swiss Federal Institute of Technology, Zurich, Switzerland).

Antibodies. The rabbit polyclonal antibodies used were against RARα, SRC-3, β-actin, CUL-1, and CUL-2 (all from Santa Cruz Biotechnologies), CUL-3 (Sigma-Aldrich), and phospho-p38 MAPK (Thr180/Tyr182) (Cell Signaling). Goat polyclonal antibodies against RBX1 were from Santa Cruz Biotechnologies. Mouse monoclonal antibodies were against FLAG-tag (Sigma-Aldrich), HA-Tag, SRC-3 (BD-Bioscience), and mono- and polyubiquitinated conjugates (Enzo Life Sciences). Mouse monoclonal antibodies recognizing SRC-3 phosphorylated at S860 were generated by immunization of BALB/c mice with synthetic phosphopeptides (3).

RNAi E3-Ubiquitin Ligase Screen. Screening was performed at the high-throughput screening facility of the Institut de Génétique et de Biologie Moléculaire et Cellulaire, using a siRNA library (4 individual siRNA per protein) targeting 111 E3 Ubiquitin Ligases and associated proteins (Flexiplate siRNA sets; Qiagen) (Dataset S1). Controls were performed with smartpool siRNAs from Dharmacon (Thermo Scientific) [siRNAs against human SRC-3 (M-003759-02) and SUG-1 (M-009484-02) and scramble siRNA] or from Qiagen [siRNAs against CUL-1 (Hs_Cul1_5), CUL-2 (Hs_Cul2_3), CUL-3 (Hs_Cul3_5), RBX1 (Hs_RBX1_5), PSMB1 (Hs_PSMB1_2), and PSMB2 (Hs_PSMB2_2)]. For each target, 3.5 pmol siRNA was reverse transfected in 5,000 MCF7 cells per 0.3 cm^2 by using Interferin (Polyplus).

All screens were performed in 96-well cell culture microplates with a particular focus on avoiding microplate edge effects. SRC-3 degradation was analyzed by immunofluorescence 3 d after siRNA transfection and 3 h after RA addition. Cells were washed, fixed with 3% paraformaldehyde, permeabilized with 0.1% Triton X-100, blocked with 2% BSA, and incubated with SRC-3 antibodies followed by ALEXAFluor 488-conjugated second antibodies (Invitrogen). The screens were achieved owing to a TECAN robotic station (for cell transfection, staining, and immunocytochemistry) and to a Caliper Twister II robotic arm coupling microplate stacks to the InCELL1000 analyzer microscope (GE LifeSciences).

Statistical Analysis of the siRNA Screens. After background-correction and interplate normalization, internal positive and negative plate controls were used to determine a threshold for cell classification. The distance from negative controls was quantified by determining the percent of control (i.e., the percentage of positive cells in the test experiment versus the negative control). After multiple testing correction, P values were determined. Then gene selection was based on the one-sided tests procedure with H0: $Xp \leq \alpha$ and H1: $Xp > \alpha$, where Xp is the percent of control estimator and α is a sensibility parameter ($\alpha \geq 1$ and $\alpha = 2$ for high stringency).

Cell Lines, Cell Proliferation, Transfection, Immunoprecipitation, and Immunoblotting. COS-1, MCF7, BT474, and MDA-MB361 cells were cultured and transiently transfected under standard conditions. After RA (10^{-7} M) addition (4), whole-cell extracts or subcellular fractions (cytosol, nucleoplasm, and chromatin) were prepared, immunoblotted, and immunoprecipitated (2, 3). Cell proliferation was analyzed by using the XTT (2,3-bis-(2-methoxy-4-nitro-5-sulfophenyl)-^{2}H-tetrazolium-5-carboxanilide) assay kit (Roche Diagnostics).

Detection of in Vivo Phosphorylated SRC-3. Cell extracts were applied to phosphoprotein purification columns (Qiagen). Column eluates containing protein peaks were concentrated and analyzed by immunoblotting (4).

Immunofluorescence Analysis and Proximity Ligation Assay (PLA). Cells were seeded onto labtek chamberslides (Fisher Scientific), proceeded as described for the RNAi screen, and incubated with the primary antibodies followed by ALEXAFluor 448- or 555-conjugated secondary antibodies or by the PLA probes (Duolink II; Eurogentec) as described (5). Images were edited by using ImageJ.

RNA isolation, quantitative RT-PCR, and chromatin immunoprecipitations (ChIP) were performed as described (2, 4). Primer sequences are available upon request.

1. Giannì M, et al. (2006) P38MAPK-dependent phosphorylation and degradation of SRC-3/AIB1 and RARalpha-mediated transcription. *EMBO J* 25:739–751.
2. Ferry C, et al. (2009) SUG-1 plays proteolytic and non-proteolytic roles in the control of retinoic acid target genes via its interaction with SRC-3. *J Biol Chem* 284:8127–8135.
3. Lalevée S, et al. (2010) Vinexinß, an atypical "sensor" of retinoic acid receptor gamma signaling: Union and sequestration, separation, and phosphorylation. *FASEB J* 24: 4523–4534.
4. Bruck N, et al. (2009) A coordinated phosphorylation cascade initiated by p38MAPK/MSK1 directs RARalpha to target promoters. *EMBO J* 28:34–47.
5. Piskunov A, Rochette-Egly C (2011) A retinoic acid receptor RARα pool present in membrane lipid rafts forms complexes with G protein αQ to activate p38MAPK. *Oncogene*, in press.

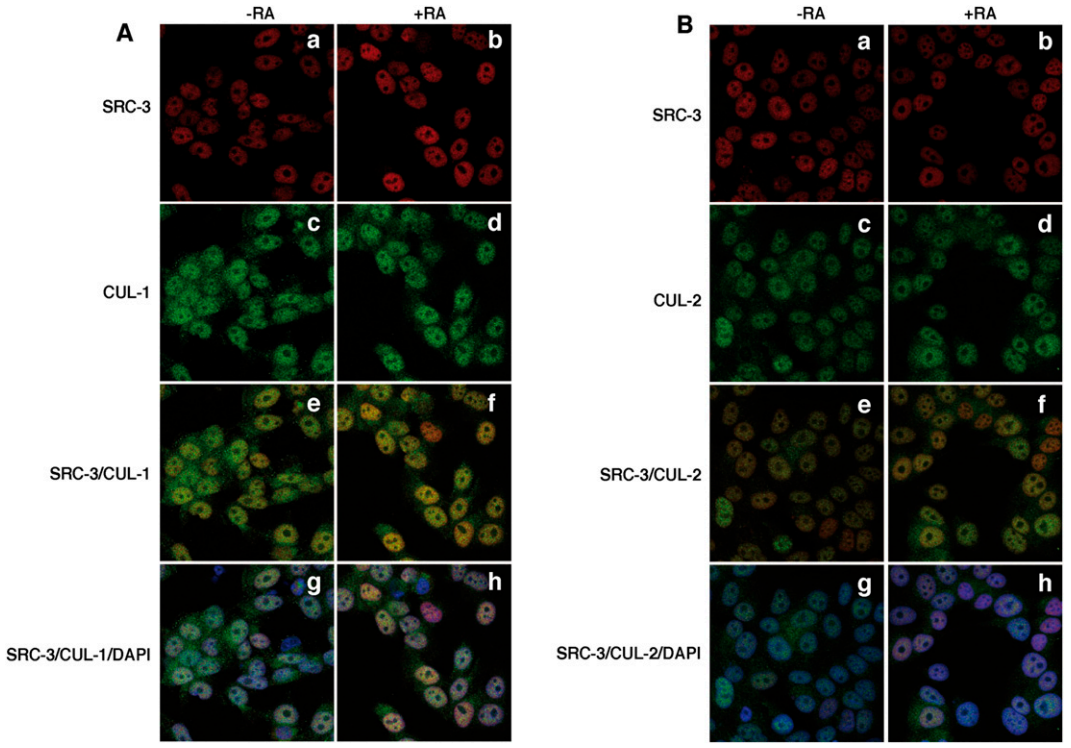

Fig. S1. The nuclear localization of CUL-1 and CUL-2 is not affected by RA. (*A*) MCF7 cells were RA-treated (*b, d, f,* and *h*) or not (*a, c, e,* and *g*) for 2.5 h, fixed, triple stained with DAPI (blue), SRC-3 antibodies (red), and CUL-1 antibodies (green), and examined by confocal microscopy. Merges overlapping the red and green (*e* and *f*) and the red, green, and blue (*g* and *h*) are shown. (*B*) Same as in *A* with CUL-2 antibodies.

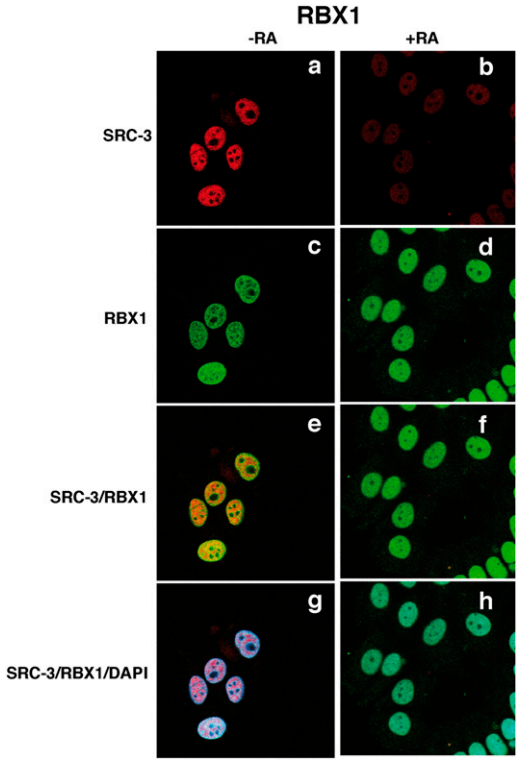

Fig. S2. The nuclear localization of Rbx1 is not affected by RA. MCF7 cells were RA-treated (*b, d, f,* and *h*) or not (*a, c, e,* and *g*) for 2.5 h, fixed, triple stained with DAPI (blue), SRC-3 antibodies (red), and Rbx1 antibodies (green), and examined by confocal microscopy. Merges overlapping the red and green (*e* and *f*) and the red, green, and blue (*g* and *h*) are shown.

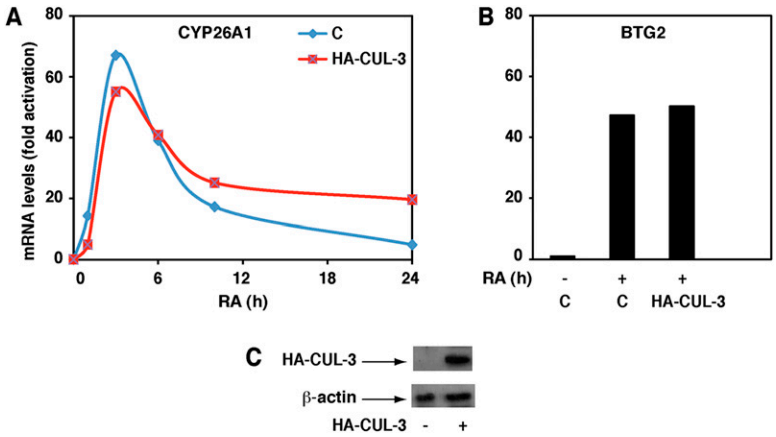

Fig. S3. The RA-induced expression of the *Cyp26A1* (*A*) and *Btg2* (*B*) genes is not affected by CUL-3 overexpression. Values are expressed as fold induction relative to untreated cells and correspond to a representative experiment among three. Overexpression efficiency was controlled by immunoblotting (*C*).

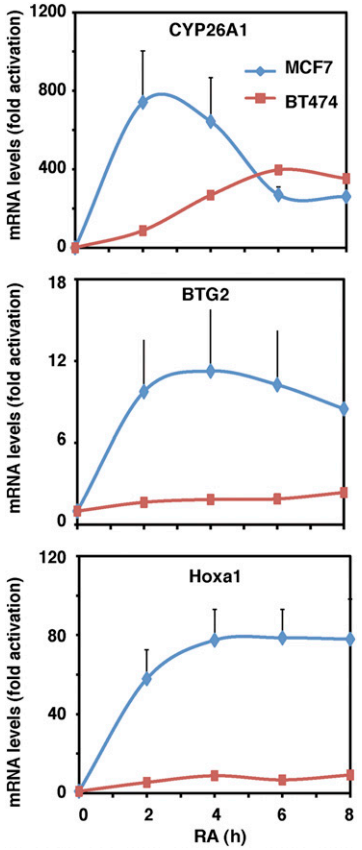

Fig. S4. Real-time RT-PCR experiments showing that in BT474 human breast cancer cells, the *Cyp26A1* (*Top*), *Btg2* (*Middle*), and *Hoxa1* (*Bottom*) genes are not induced, compared with MCF7 cells.

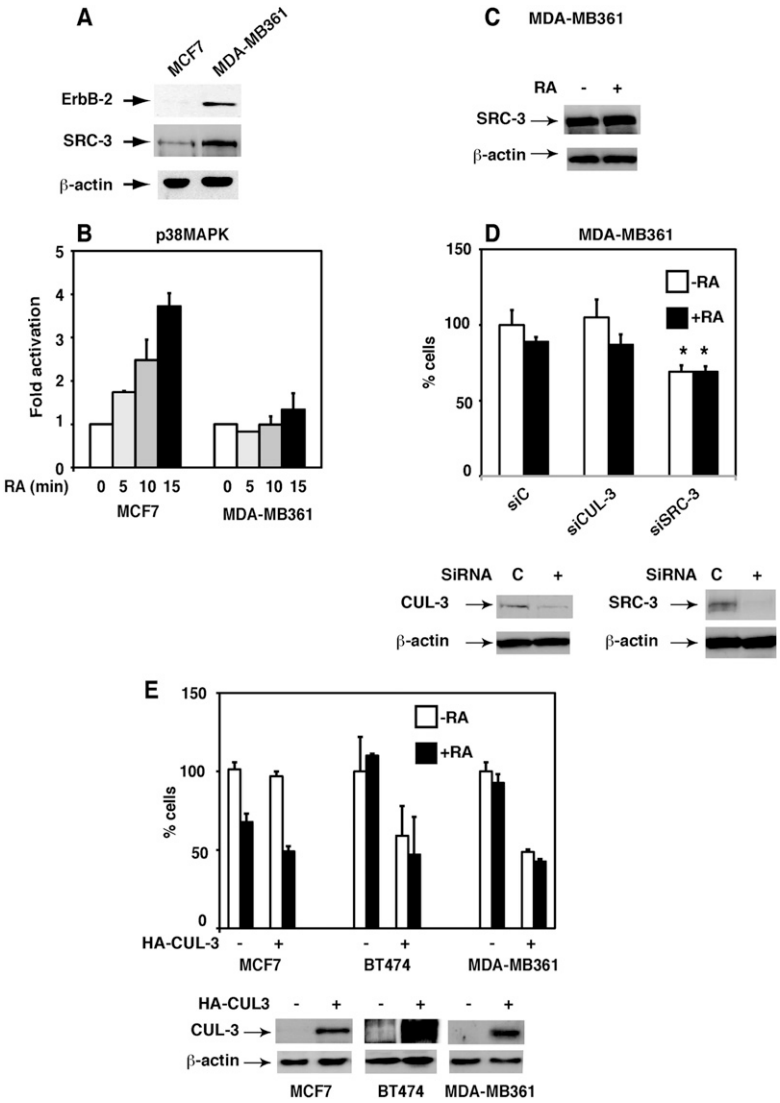

Fig. S5. In RA-resistant MDA-MB361 cells, SRC-3 is not degraded. (*A*) Immunoblots showing the overexpression of erbB-2 and SRC-3 in MDA-MB361 cells, compared with MCF7 cells. (*B* and *C*) In MDA-MB361 cells, p38MAPK is not activated and SRC-3 is not degraded. (*D*) The growth of MDA-MB361 cells is not affected by RA nor by knockdown of CUL-3 but is decreased upon knockdown of SRC-3 (*Upper*). The efficiency of knockdown was checked by immunoblotting (*Lower*). The results are the mean ± SD of two distinct experiments performed in quadruplate. Statistically significant differences were indicated (*$P < 0.05$, control versus siRNA). (*E*) The growth of BT474 and MDA-MB361 cells is markedly decreased upon overexpression of CUL-3 (*Upper*). Overexpression efficiency was checked by immunoblotting (*Lower*). The results are the mean ± SD of two distinct experiments performed in quadruplate.

Other Supporting Information Files

Dataset S1 (XLSX)